Finite amplitude wave propagation in solid and liquid ^{4}He

A. Hikata, H. Kwun, and C. Elbaum
Metals Research Laboratory, Brown University, Providence, Rhode Island 02912
(Received 6 November 1979)

The amplitude response (i.e., relation between input and output amplitudes of a wave transmitted through a medium) of 10-MHz longitudinal wave is investigated in hcp and bcc solid ^{4}He as well as normal fluid and superfluid ^{4}He. In all four phases the acoustic saturation in the amplitude response curve was observed. The results are well described by an equation for amplitude loss based on second-harmonic generation. The nonlinear parameter β of these phases was evaluated. It is found that the magnitude β in solid ^{4}He is comparable to that of classical solids. Dislocation contributions to the amplitude response were also investigated and were ruled out as a significant source of the observed effects. It is concluded, therefore, that the large nonlinear amplitude response, which leads to saturation observed in solid ^{4}He should be attributed to the unusually large compressibility, i.e., small elastic constants (second order), which, in turn, induces in solid ^{4}He much larger strain amplitudes for a given applied stress than in ordinary solids.

I. INTRODUCTION

One of the characteristics of ultrasonic wave propagation in nonlinear media is the waveform distortion, or equivalently, the generation of higher-harmonic waves. As the amplitude of the fundamental wave increases, the effect of this conversion to higher harmonics becomes significant and results in a nonlinear amplitude response of the wave; i.e., the attenuation of the fundamental wave becomes amplitude dependent. This amplitude-dependent attenuation is often referred to as "finite amplitude losses." With further increase of the wave amplitude, a phenomenon called "saturation" takes place, whereby the amplitude of the transmitted wave measured at a given distance from the source approaches a limiting value; i.e., the signal amplitude received becomes essentially independent of the source strength. Although there are several experimental reports on finite amplitude losses and saturation for the cases of liquids[1–4] and gases,[5] as far as the authors are aware, none has been reported for solids. In this paper, we show that in liquid ^{4}He (both normal and superfluid phase) and in particular also in solid ^{4}He (both bcc and hcp phase) these two effects are observed.

These results are analyzed in the frame of continuum mechanics, and the nonlinear parameters are evaluated. It is found that the magnitude of the nonlinear parameters in ^{4}He crystals is comparable to that of classical crystals. Dislocation contributions to the amplitude dependence were also investigated and were ruled out as a significant source of the observed effects. We conclude, therefore, that the large amplitude dependence, which leads to saturation observed in solid ^{4}He should be attributed to the unusually small elastic constants (second order) which, in turn, induce much larger strain amplitudes in solid ^{4}He than in ordinary solids for a given applied stress.

II. EXPERIMENTAL PROCEDURE

The sample holder, a cell made out of brass whose outer dimensions are approximately $2 \times 2 \times 3$ cm^3 is immersed in a liquid-^{4}He bath. On the inner faces of the side walls of the cell, three ultrasonic transducers are mounted, two facing each other 1 cm apart and the third perpendicular to the other two. Those two transducers are used for, respectively, transmitting and receiving ultrasonic waves for the amplitude-dependence measurements, and the third is used for the purpose of superimposing a dynamic bias stress[6] on the sample. These are all $LiNbO_3$-coaxially-plated transducers of fundamental frequency of 10 MHz (active plating is 0.3 cm in diameter). The cell is pressurized to a desired pressure through a fill line, and is maintained at a predetermined temperature by controlling the pumping speed of the ^{4}He bath. Radio-frequency pulses of 10 MHz (pulse width of ~ 3 μsec, repetition rate of ~ 20 Hz) are applied to the transmitting transducer through a step attenuator. The signals of the wave thus generated in the sample are processed through the receiving transducer, another step attenuator, a tuned receiver, a peak detector, and chart recorder. The step attenuator in the transmitting side is for changing the input amplitude P_{10} by a known amount. The step attenuator in the receiving side is for minimizing the error caused by nonlinearity which might exist in the receiver, by maintaining an approximately constant amplitude of

the input to the receiver. The overall error of the measurement was ±5%. The received signal amplitude P_1 is then plotted on a log-log scale as a function of P_{10} (amplitude response curve). Both P_1 and P_{10} are measured relative to their respective initial values, which are arbitrary. The same sample holder is used for liquid- and solid-^{4}He experiments.

III. RESULTS AND DISCUSSION

A. Liquid ^{4}He

Typical amplitude response curves for liquid ^{4}He are shown in Fig. 1 (obtained at $T=1.74$ K, $P=27.6$ atm for superfluid, and at $T=1.90$ K, $P=32.5$ atm for normal fluid). In the absence of amplitude dependence of the attenuation the relation between P_1 and P_{10} is governed by the expression

$$P_1 = P_{10}e^{-\alpha x}\sin(\omega t - kx) \ , \tag{1}$$

and in a log-log plot it should yield a straight line of slope one, as indicated by a dashed line in Fig. 1. In the above, α is the attenuation coefficient for "small-amplitude" waves caused by viscosity, etc., which is considered to be amplitude independent, x is the propagation distance of the wave, ω is the frequency, and k is the wave vector. As can be seen, however, actual data depart from the straight line, indicating the existence of extra attenuation at high amplitudes.

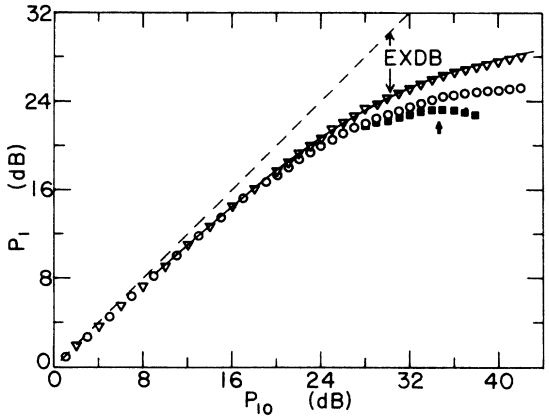

FIG. 1. Received signal amplitude P_1 of 10-MHz wave as a function of input signal amplitude P_{10} (amplitude response curve) in liquid ^{4}He. The differences between the slope one line (dashed straight line) and the data points correspond to EXDB. The solid curve represents the calculated values obtained by Eq. (6) for both normal fluid and superfluid. The difference between the two cases is not distinguishable on the scale of the drawing. ▽: superfluid at $T=1.74$ K and $P=27.6$ atm; ○: normal fluid at 1.90 K and $P=32.5$ atm; ■: normal fluid as above except that the repetition rate of the ultrasonic pulses is increased by a factor of 10, to 200 Hz. The arrow indicates the onset of the instability.

This extra attenuation corresponds to the "finite amplitude loss" mentioned earlier and is designated by EXDB (extra dB). As the input amplitude increases, the EXDB increases and P_1 tends toward a limiting value; i.e., it shows the effect of saturation.

The analysis of nonlinear wave propagation has a long history.[7,8] Here, we use the amplitude-loss equation[1,5,9] given by

$$\frac{dP_1}{dx} = -\alpha P_1 - \frac{\beta k}{2\rho_0 c_0^2} P_1^2 \ . \tag{2}$$

In the above β is the nonlinear parameter of the medium, and is defined by

$$\beta = B/2A + 1 \ , \tag{3}$$

where $A\,(=\rho_0 c_0^2)$ and B are the coefficients of a Taylor-series expansion of pressure P_1 in terms of density change $(\rho-\rho_0)/\rho_0$ defined by

$$P_1 = A\left(\frac{\rho-\rho_0}{\rho_0}\right) + \frac{1}{2}B\left(\frac{\rho-\rho_0}{\rho_0}\right)^2 + \cdots \ . \tag{4}$$

The solution of Eq. (2) with the initial condition

$$P_1 = P_{10}|_{x=0}$$

is

$$P_1 = P_{10}e^{-\alpha x}[1 + (1-e^{-\alpha x})/2\alpha\bar{x}]^{-1} \tag{5}$$

or, in terms of EXDB, expressed by X,

$$X = 20\log_{10}[1 + (1-e^{-\alpha x})/2\alpha\bar{x}] \ , \tag{6}$$

where $\bar{x}$ is the discontinuity distance given by

$$\bar{x} = 1/\beta\epsilon k \tag{7}$$

with $\epsilon = P_{10}/\rho_0 c_0^2$ (acoustic Mach number). The first term on the right-hand side of Eq. (2) corresponds to the rate of amplitude decrease caused by the small-amplitude attenuation, and the second term corresponds to that caused by generation of second harmonic.[10] In the temperature range not too close[11] to the λ transition, $|(T-T_\lambda)/T_\lambda| \gtrsim 10^{-2}$, B/A can be estimated by[7]

$$\frac{B}{A} = 2c_0\rho_0\left(\frac{\partial c}{\partial p}\right)_{T,\rho_0} + \frac{\gamma T c_0}{C_p}\left(\frac{\partial c}{\partial T}\right)_{P,\rho_0} \ , \tag{8}$$

where γ is the thermal expansion coefficient, and C_p is the specific heat under constant pressure. [It turns out that the second term on the right-hand side of Eq. (8) is small and can be neglected.] For the experimental conditions mentioned above, $\rho_0=0.178$ g/cm^3, $c_0=3.60\times10^4$ cm/sec, and $(\partial c/\partial p)_T \simeq 2.9\times10^{-4}$ cm/sec dyn cm^2 for superfluid[12,13] and $\rho_0=0.181$ g/cm^3, $c_0=3.85\times10^4$ cm/sec, and $(\partial c/\partial p)_T \simeq 3.57\times10^{-4}$ cm/sec dyn cm^2 for the normal fluid. With these values, one obtains $\beta_{\text{super}}=2.86$, $\beta_{\text{normal}}=3.50$, $\bar{x}_{\text{super}}=4.62\times10^4/P_{10}$ cm, and $\bar{x}_{\text{normal}}$

$=4.69\times10^4/P_{10}$ cm. With $x=1$ cm and measured value of $\alpha=0.4$ Np/cm for both superfluid and normal fluid, P_1 or EXDB can be calculated as a function of P_{10}. Since only relative values of P_1 and P_{10} are obtainable in the present experiments, the origin of the coordinates for the data points is arbitrary. By adjusting the position of the origin, therefore, one can test the fit of Eq. (5) or Eq. (6) to the data. The solid curve in Fig. 1 is the result of such fittings for both normal fluid and superfluid. [The difference in the calculated values between the two cases is not distinguishable on the scale of the drawing. This is accidental and is due to the fact that in Eq. (7) for $\bar{x}$, the larger β in the normal fluid is compensated by a larger sound velocity for the higher pressure of the measurements in this phase.] As can be seen, the fit is quite good for the superfluid state. In the normal state, the EXDB increases more rapidly at high amplitudes than predicted by Eq. (6). In the superfluid state, with this fitting procedure, one can estimate the absolute values of P_{10}. The value thus obtained is 4×10^5 dyn/cm^2 for the maximum amplitude used in this study which corresponds to 42 dB in Fig. 1.

When P_{10} is further increased, in the normal state, the ultrasonic echo shape becomes unstable; i.e., it changes with time. The effect sets in at lower amplitudes if the pulse width or repetition rate are increased. For example, the data points indicated by solid squares were obtained under the same condition as those of open circles, except that the repetition rate was increased by a factor of 10 (to 200 Hz). The onset of the instability detected on the oscilloscope screen is indicated by an arrow. The effect may be due to such causes as streaming[14] or cavitation[15] in the sample, and may also be responsible for the departure of the data from the theoretical prediction. In the superfluid state, on the other hand, such an instability was not observed within the experimental conditions of the present study.

Without knowing the absolute value of P_{10}, it is still possible to deduce the ratio $\beta_{\text{normal}}/\beta_{\text{super}}$ from the data. Using the values of EXDB evaluated below the 24-dB point for P_{10} in Fig. 1, and the same values for ρ_0, c_0, and α mentioned above, one obtains

$$(\beta_{\text{normal}}/\beta_{\text{super}})_{\text{expt}}\simeq 1.35 \ .$$

A similar evaluation of EXDB at a larger amplitude of P_{10} (32 dB) gives a ratio $\sim$1.59. These values may be compared with the value calculated above

$$(\beta_{\text{normal}}/\beta_{\text{super}})_{\text{calc}}\simeq\frac{3.50}{2.86}=1.21 \ .$$

B. Solid ^{4}He

Without altering the experimental arrangements, ^{4}He crystals were grown in the cell, and the amplitude dependences were investigated in the same manner as in the liquid case. We could not grow crystals with predetermined orientations, and thus the direction of the wave propagation generally did not coincide with a high-symmetry crystallographic axis. Data were taken for the crystals whose sound velocity ranged from 5.00×10^4 cm/sec to 5.27×10^4 cm/sec in the hcp phase and from 5.15×10^4 cm/sec to 5.40×10^4 cm/sec in the bcc phase.

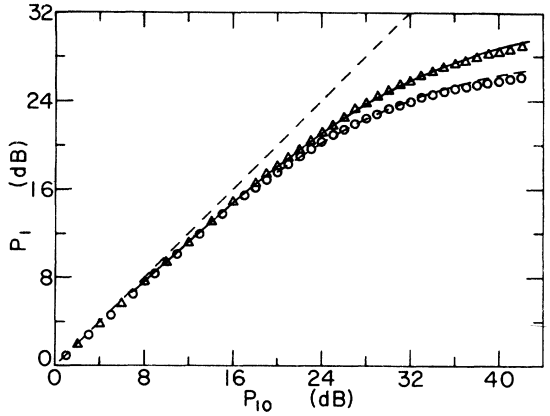

FIG. 2. Amplitude response curve in solid ^{4}He. Δ: hcp phase at $T=1.67$ K, $P=32.5$ atm, and $c_0=5.06\times10^4$ cm/sec; ○: bcc phase at $T=1.62$ K, $P=27.6$ atm, and $c_0=5.40\times10^4$ cm/sec. The solid and dashed curves represent the calculated values obtained by Eq. (6) for hcp and bcc phases, respectively. As in Fig. 1, the dashed straight line of slope one is used as the reference for EXDB.

Typical results for hcp (taken at $T=1.67$ K, $P=32.5$ atm, $c_0=5.06\times10^4$ cm/sec, $\rho_0=0.195$ g/cm^3) and bcc (at $T=1.62$ K, $P=27.6$ atm, $c_0=5.40\times10^4$ cm/sec, and $\rho_0=0.190$ g/cm^3) are shown in Fig. 2. [Also shown in this figure are the values calculated from Eq. (6) for hcp crystals by the solid curve and for bcc crystals by the dashed curve, to be discussed later.] As can be seen, and to our surprise, the results are very similar to the case of liquid ^{4}He shown in Fig. 1. This suggests that the origin of the observed amplitude dependence in solid ^{4}He is also the generation of the second harmonics. Two sources of harmonic generation are readily envisaged; i.e., the lattice anharmonicity and the oscillation of dislocations. Besides the generation of harmonic, dislocations are known to be responsible for amplitude-dependent attenuation in ordinary solids. Therefore, in the next section, the likelihood of dislocations being the cause of the observed amplitude dependence is examined. This is followed by a discussion of the effects of intrinsic lattice anharmonicity.

1. Dislocation contribution

Motion of dislocations can cause amplitude-dependent attenuation in many ways. Among vari-

ous processes, the most often cited mechanism is the breakaway[16] (unpinning) of dislocations from weak pinning points (point defects). The functional form of the dependence of the attenuation on amplitude is complicated. Generally, as the input amplitude is increased, the attenuation starts increasing rather sharply at a certain amplitude. With further increases of the amplitude, the rate of attenuation increase decreases, and eventually goes into a plateau or even goes through a maximum. The appearance of the plateau or the maximum at high amplitudes is the consequence of the exhaustion of pinning points from which dislocations can break away.[17] A schematic diagram of the attenuation-amplitude relation (α-P_{10} diagram) is shown in Fig. 3(a). If one converts the α-P_{10} relation into the amplitude response relation (P_1-P_{10} relation), the resulting diagram would be of the form shown in Fig. 3(b). When P_{10} is small (A-B), P_1 falls on the straight line of slope one (A'-B'). At $P_{10}=B$, amplitude dependence appears in the attenuation. In the P_1-P_{10} diagram this corresponds to the sharp departure of P_1 from the slope one line at B'. The plateau in the α-P_{10} diagram corresponds in the P_1-P_{10} diagram to the slope one line $C'D'$. When α decreases after passing through the plateau (D-E), the corresponding P_1 must approach the original straight line of slope one (D'-E'). Such behavior of P_1, however, has never been observed in the present investigation. This suggests that the dislocation contribution through the unpinning mechanism is negligible in the present study.

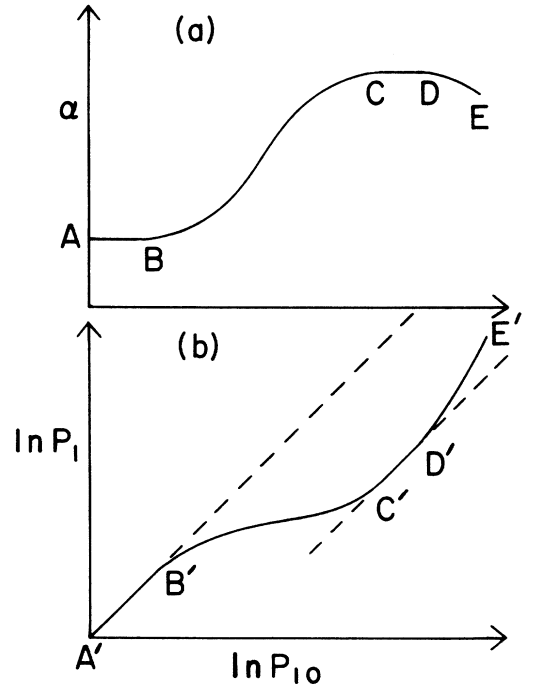

FIG. 3. (a) Schematic diagram of attenuation α as a function of input amplitude P_{10}. A-B, small amplitude (amplitude independent) attenuation; B-C, amplitude-dependent attenuation; C-D, plateau; and D-E, attenuation decrease due to exhaustion. (b) Corresponding amplitude response diagram (schematic). The slope-one lines are represented by the two dashed lines.

In order to test further the extent of dislocation contribution, dynamic bias stress experiments were carried out. The bias stress test[6] consists of superimposing a wave of large enough amplitude to unpin dislocations, while the measuring wave (of small amplitude) is propagated in the sample. If the bias stress induces dislocation unpinning, the small amplitude attenuation α_d should change (increase or decrease depending on the frequency, magnitude of the damping, and the segment length). Using the third transducer placed perpendicular to the pair of the measuring transducers, a large-amplitude wave of 10 MHz (comparable to the maximum amplitude P_{10} shown in Fig. 1) is applied. In the present study small but measurable changes in α were observed in both hcp and bcc phases. The characteristics of the change, $\Delta\alpha$, however, are quite different from the ones attributed to dislocation unpinning and observed previously[6,18,19] in ordinary solids. We denote by Δt the delay time of the trigger time of the bias wave. Since the magnitude of the effect should depend critically on the amplitude of the bias wave, because of the catastropic nature of the breakaway process, and since the wave amplitude decays due to the attenuation, the behavior of $\Delta\alpha$ as a function of Δt for a given bias stress wave should be as follows: As Δt is increased starting from zero, full magnitude of $\Delta\alpha$ should be observed during the initial time period corresponding approximately to the pulse width of the bias wave ($\sim$30 μsec) and then decrease rather sharply. In fact this was the characteristic of $\Delta\alpha$ observed in ordinary solids. The experiments carried out to check this effect in solid ^{4}He revealed that, contrary to the case of ordinary solids, no significant changes in $\Delta\alpha$ were observed for Δt from zero up to at least 50 msec. If the change, $\Delta\alpha$, is the consequence of the breakaway process, this finding implies that once a dislocation breaks away from pinning points, it stays unpinned long after the bias stress has decayed out, which is very unlikely.[20] Therefore, we conclude that the bias stress effect attributable to the dislocation breakaway process is practically absent in solid ^{4}He. The absence of the bias stress effect is thought to be due to a lack of effective pinning points from which dislocations can break away. The only impurities which can exist in solid ^{4}He are ^{3}He atoms. Although we cannot determine the concentration of ^{3}He atoms in our ^{4}He crystals, the starting material has a concentration[21] of ^{3}He not in excess of 1 ppm. Other candidates as the pinning agent (in ordinary solids) are vacancies. However, according to a

study of dislocation pinning processes by Iwasa and Suzuki[22] this is not the case in solid ^{4}He. These authors investigated amplitude dependence of attenuation in the temperature range from 0.12 to 1.8 K and with 10-, 30-, and 50-MHz longitudinal waves. According to their results, amplitude dependence of attenuation occurred in solid ^{4}He samples which contained a small amount of ^{3}He atoms as impurities ($\sim$30 ppm). The effect disappeared at temperatures of $\sim$1 K and above. In pure ^{4}He crystals,[23] on the other hand, no amplitude dependence was detected at all temperatures investigated. This finding implies that vacancies are either very strong or completely ineffective pinning points. Judging from the trend found in ordinary solids[24] that vacancies are less effective as pinning points of dislocations than impurities, it is natural to infer that vacancies in solid ^{4}He are not effective pinning agents in the temperature and frequency range studied here.

Another possible cause of the amplitude dependence is the generation of harmonics by large amplitude oscillations of dislocation segments.[25] Here, it is assumed that no breakaway from, nor dragging of pinning points takes place. Pinning of dislocations by intersecting dislocations, for example, provides such a pinning situation. We assume that the dislocation segment is straight at the outset, and the Peierls stress[26] is negligible. The equation of motion of such a dislocation segment under the influence of an oscillatory stress can be treated by analogy with a vibrating string.[16] The restoring force appearing in the equation of motion is the line tension of the dislocation arising from the energy difference between the displaced (bowed out) and the straight dislocation configurations. Because of the symmetry requirement (i.e., deviations from the straight configuration should be the same for equal positive and negative stresses), the first nonlinear term which appears in the restoring force term is proportional to $f''f'^2$ where $f'=\partial\xi/\partial\eta$ (η is the coordinate on the dislocation segment and ξ is the displacement of the segment; see Fig. 4). Since the displacement of dislocations, ξ, is proportional to P_1 in this approximation,

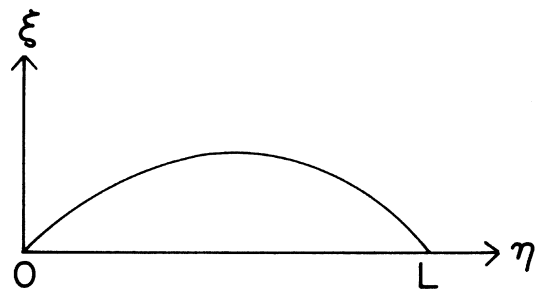

FIG. 4. Schematic representation of displacement of dislocation segment which has length L and is pinned at both ends.

the dominant harmonic generated from such a nonlinear equation of motion is the third harmonic instead of the second harmonic. As mentioned earlier, the behavior of the amplitude response of solid ^{4}He is similar to that of liquid ^{4}He, which is found to be consistent with the second-harmonic generation and not of the third-harmonic generation.[10] Therefore, the contribution of harmonic generation by dislocations to the observed results can be considered very small.

Thus the most plausible dislocation mechanisms for the amplitude dependence of attenuation, the breakaway process and the dislocation generation of harmonics, are ruled out as the cause of the observed results. This does not necessarily mean that dislocations do not contribute to the amplitude independent attenuation α_d. In fact, at least in hcp crystals, the attenuation of small amplitude waves increased drastically[27] when the samples were deformed plastically by static compressional stresses. This increase has been attributed to an increase in the dislocation density.

2. *Lattice anharmonicity*

The observed results are now discussed in terms of the second-harmonic generation by lattice anharmonicity. The analysis can be carried out in a manner similar to that of liquid ^{4}He. The relation corresponding to expression (4) in solids is the expansion in a Taylor series of strain energy density in terms of deformation tensor components. The expression for the general case is very lengthy, and since we do not distinguish crystal orientations, such a formula is not useful here. Following Brugger's[28] convention, the stress-strain relation in the one-dimensional case is given by

$$\sigma = K_2\left(\frac{\partial u}{\partial x}\right)+\frac{1}{2}(K_3+3K_2)\left(\frac{\partial u}{\partial x}\right)^2+\cdots , \quad (9)$$

where K_2 and K_3 are taken as "effective" second- and third-order elastic constants and consist of, respectively, combinations of the second- and third-order elastic constants. With this definition, the nonlinear parameter β_{solid} becomes

$$\beta_{\text{solid}}=\tfrac{3}{2}+K_3/2K_2 .$$

With the known values of ρ_0 and measured values of c_0 and α the relative values of β_{solid} to β_{super} are calculated. Here, however, the initial amplitude P_{10} must be adjusted by a factor determined from the difference in the acoustic impedance between the liquid and the solid ^{4}He. The values thus obtained from the data of Fig. 2 are

$$\beta_{\text{hcp}}/\beta_{\text{super}}=1.93$$

and

$$\beta_{\text{bcc}}/\beta_{\text{super}}=3.18 .$$

The fitting of the expression (6) with these values is shown by the solid curve for hcp crystals and by the dashed curve for bcc crystals, as mentioned earlier in Fig. 2. As can be seen, the fit is excellent.

If we take for β_{super} the value calculated from the expression (7), β_{hcp} and β_{bcc} can be determined. These values differ somewhat for crystals of different orientations (i.e., crystals having different sound velocity). A list of these values for four cases is shown in Table I. It is difficult, however, to extract from this table a trend which might exist between β and c_0. In all cases, β_{solid} is larger than β_{liquid}. As far as we are aware, no other investigations have been reported of the nonlinear coefficient in both liquid and solid phases of the same material. Therefore, no comparisons with other cases are possible.

From these values of β one can estimate the ratio K_3/K_2. It ranges from 8 to 11 for hcp and from 11 to 15 in bcc crystals. It should be mentioned that the values of β deduced here are absolute values and we have no way of distinguishing their sign. If β is negative, then the range for K_3/K_2 should be read $-11 \gtrsim K_3/K_2 \gtrsim -14$ for hcp and $-14 \gtrsim K_3/K_2 \gtrsim -18$ for bcc ^{4}He. These ratios can be compared with those in other solids. The values calculated from various sources are listed in Table II.[29–36] It is apparent from the table that the values obtained for solid ^{4}He in this study are large but not extraordinary. This means that the nonlinearity of ^{4}He crystals is of the same order of magnitude as that of ordinary solids. The reason why the former exhibits much larger nonlinear effects in wave propagation than the latter is that the sound velocity and the density are each approximately one order of magnitude smaller in solid ^{4}He than in ordinary solids (i.e., the second-order elastic constants are roughly three orders of magnitude smaller). Therefore, for a given applied (and experimentally available) stress wave

TABLE I. A list of measured values of attenuation α, sound velocity c_0, and corresponding values of $\beta_{solid}/\beta_{super}$ for four different samples of bcc and hcp solid ^{4}He.

	α (Np/cm)	c_0 (10^4 cm/sec)	$\beta_{solid}/\beta_{super}$
	0.3	5.4	2.76
	1.12	5.15	3.04
bcc	0.45	5.26	2.42
	0.39	5.33	2.58
	0.6	5.06	1.93
	0.46	5.03	1.85
hcp	1.2	5.27	2.29
	0.69	5.0	2.36

TABLE II. Values of K_3/K_2 for various solids.

K_3/K_2	Cu	Au	Ag	NaCl	KCl	LiF	MgO	Ge	Si	$SrTiO_3$	Suprasil
$\langle 100 \rangle$ $\frac{C_{111}}{C_{11}}$	−8.25	−8.99	6.80	−17.2	17.35	−12.48	−16.48	−5.68	4.98	−15.74	8.59
$\langle 110 \rangle$ $\frac{\frac{1}{4}(C_{111}+3C_{112}+12C_{166})}{\frac{1}{2}(C_{11}+C_{12}+2C_{44})}$	−14.18	−13.96	−16.26	−9.89	−9.19	−9.73	1.93	−12.40	−7.60	8.26	
$\langle 111 \rangle$ $\frac{\frac{1}{9}(C_{111}+6C_{112}+12C_{144}+24C_{166}+2C_{123}+16C_{456})}{\frac{1}{3}(C_{11}+2C_{12}+4C_{44})}$	10.81	−11.47	−11.38	−4.63	−4.26	−6.49	4.17	−11.50	−6.52	−8.32	
Ref.	29	30	30	31	31	31	32	33	34	35	36

amplitude, one order of magnitude larger strains are induced in solid ^{4}He even after the adjustment is taken into account for the acoustic impedance mismatch between transducers and the sample.

As in the case of liquid ^{4}He in the normal state, an instability occurs in the solid when the input energy is increased beyond a certain value. Since streaming or cavitation cannot be considered in solids, we attribute this effect to local melting of the surface layer of the sample in contact with the transducer. This was confirmed by shear-wave experiments where the effect was found to be greatly enhanced because of the inability of the liquid (the melt) to support shear-wave propagation.

IV. COMPARISON WITH OTHER INVESTIGATORS' RESULTS

A. Liquid ^{4}He

As far as the authors are aware, there are no reports concerning the amplitude dependence of attenuation in liquid ^{4}He. The values of the nonlinear parameter calculated above are comparable to those of other liquids.[7]

B. Solid ^{4}He

Tsuruoka and Hiki[37] (hereafter indicated by TH) reported the amplitude dependence of ultrasonic attenuation of 5-MHz longitudinal waves in hcp crystals measured at 1.70 K (molar volume 20.5 cm^3). The behavior of the logarithmic decrement $\Delta(=2\pi c_0\alpha/\omega)$ reported by these authors may be summarized as follows: (a) At low amplitudes Δ remains constant; (b) at sufficiently large amplitudes, Δ increases rapidly with increasing amplitude; (c) eventually with further increase of amplitude, Δ levels off (shows a plateau); (d) no hysteresis effect is observed when the direction of the amplitude change is reversed; and (e) the amplitude dependence depends on the crystallographic orientations. The main difference between their results and ours is in item (c) above, i.e., the occurrence of saturation in the attenuation, instead of in the amplitude P_1. If their results are converted into the amplitude response (P_1-P_{10}) diagram (referring tc Fig. 3), the characteristic would be a curve represented by $A'B'C'D'$. As mentioned before, our data have never shown such behavior. This means that either the two groups are investigating different phenomena or one of the groups' results are incorrect. We present the following argument.

The method of attenuation measurements used by TH consists of matching calibrated exponential curves to the echo train. When the attenuation becomes amplitude dependent, however, use of such a method is no longer justifiable, simply because the decay of the echo train is not exponential by definition. Nonetheless, if this approach is still used, at sufficiently high amplitudes the heights of all the echoes become insensitive to the amplitude of the input signal, because of the saturation effect, as demonstrated in the present work. It follows that the measured attenuation becomes amplitude independent. Therefore, the method used by TH to obtain data is inappropriate for studying highly nonlinear media and is apt to lead to incorrect conclusions concerning the attenuation mechanism.

The distance x at which the data are taken relative to the discontinuity distance $\bar{x}$ [Eq. (7)] determines EXDB. Although the frequency ω they used is one-half that of our experiments and the resulting $\bar{x}$ is twice our value, the distance x to the first echo in their experiment is also approximately twice that of ours. Therefore, the susceptibility to the saturation at equal amplitude must at least be comparable in both cases. The magnitude of the amplitude dependence also depends on the distance x. Since x in their case is ambiguous (it depends on which echoes were chosen), it is meaningless to compare the magnitudes.

It should be mentioned also that the mechanism TH proposed to explain the amplitude dependence, i.e., the dislocation-jog-dragging mechanism, is not consistent with our experimental findings, as discussed below. The jog-dragging mechanism is meaningful only if the jogs in motion experience a larger Peierls stress than the dislocation segments moving on the primary slip systems. In hcp crystals the basal plane is considered to be the primary slip plane, while the jogs are not in the primary slip system and the above condition can be fulfilled. In bcc crystals on the other hand, the primary slip systems usually consist of $\langle 111 \rangle$ directions, and at least several different crystal planes containing those directions. Thus the jogs can also lie on primary slip systems. If the jog mechanism is the main cause of the amplitude dependence, one would expect, therefore, a marked difference to appear between the P_1-P_{10} relations for hcp and bcc crystals. As shown in Fig. 2, our experimental findings indicate that this is not the case.

The argument presented above, therefore, suggests that the jog mechanism TH proposed is not the major cause of the amplitude-dependent attenuation observed in this investigation.

Iwasa and Suzuki's[22] results, mentioned earlier, seem to be consistent with the breakaway mechanism of dislocations from pinning points (^{3}He atoms), as these authors postulated. Although comparison with the present results should not be made, since we have not investigated the effect of impurities nor of temperatures below 1.5 K, the absence of the amplitude dependence of attenuation in pure ^{4}He they found is not necessarily in conflict with the present

results. The reason for this discrepancy may lie in the difference in the maximum amplitude used in the experiments. Unlike in the cases of TH and of the present study, they used quartz transducers instead of $LiNbO_3$. In fact, their maxmimum amplitude was approximately one order of magnitude smaller than ours and too small to observe the lattice anharmonicity studied here.

V. CONCLUSIONS

The anharmonicities observed by means of amplitude-dependent propagation of 10-MHz longitudinal waves are of comparable magnitudes in four phases of ^{4}He, i.e, superfluid, normal fluid, hcp solid, and bcc solid. The origin of the amplitude dependence is primarily the generation of the second harmonic due to the intrinsic anharmonicity, and the experimental results on all four phases can be described by Eq. (2). Dislocation contributions to the amplitude dependence of the attenuation in the solids seem to be negligible. The ratios of the third-order elastic constants to the second-order elastic constants (K_3/K_2) in solid ^{4}He are of the same magnitude as those of ordinary solids. The fact that solid ^{4}He exhibits unusually large amplitude dependence as a solid is due to the smallness of the sound velocity, or, equivalently, the smallness of the second-order elastic constants.

One final remark should be made. It is often said[38,39] that solid ^{4}He is "very anharmonic." The notion of "very anharmonic" stems probably from the fact that the thermal expansion coefficients of solid ^{4}He are approximately three orders of magnitude larger than those of ordinary solids at approximately the same reduced temperature, T/Θ_D, where Θ_D is the Debye temperature. The thermal expansion coefficient γ is related to the Grüneisen parameter γ_G through the macroscopic relation

$$\gamma = \gamma_G C_v / 3E \ ,$$

where C_v is the specific heat under constant volume, and E is the bulk modulus. As shown in this study, the anharmonicity of solid ^{4}He is comparable with those of ordinary solids. Therefore, what makes γ large is not the Grüneisen parameter γ_G (which represents anharmonicity) but the large compressibility, i.e., the smallness of the bulk modulus E. One should not confuse a solid of "large anharmonicity" with a very compressible solid of ordinary anharmonicity.

ACKNOWLEDGMENTS

This work is supported in part by the NSF under Grant No. DMR77-12249 and through the Materials Research Laboratory of Brown University. The authors thank Professor R. T. Beyer, Professor P. J. Westervelt, and Professor I. Rudnick for valuable suggestions. The authors are especially grateful to Dr. F. Tsuruoka and Professor Hiki of Tokyo Institute of Technology, and Dr. I. Iwasa and Professor H. Suzuki of Tokyo University for providing their manuscripts prior to publication.

[1]K. A. Naugol'nykh and E. V. Romanenko, Sov. Phys. Acoust. 4, 202 (1958).
[2]F. E. Fox and W. A. Wallace, J. Acoust. Soc. Am. 26, 994 (1954).
[3]W.W. Lester, J. Acoust. Soc. Am. 40, 847 (1966).
[4]J. A. Shooter, T. G. Muir, and D. T. Blackstock, J. Acoust. Soc. Am. 55, 54 (1974).
[5]D. A. Webster and D. T. Blackstock, J. Acoust. Soc. Am. 62, 518 (1977).
[6]A. Hikata, R. A. Johnson, and C. Elbaum, Phys. Rev. B 2, 4856 (1970).
[7]R. T. Beyer and S. V. Letcher, *Physical Ultrasonics* (Academic, New York, 1969).
[8]O. V. Rudenko and S. I. Soluyan, *Theoretical Foundations of Nonlinear Acoustics* (Consultants Bureau, New York, 1977).
[9]J. F. Bartram, J. Acoust. Soc. Am. 52, 1042 (1972).
[10]H. M. Merklinger, H. O. Berktay, and M. H. Safar [in *Proceedings of the Symposium on Finite-Amplitude Wave Effects in Fluids, Copenhagen, 1973*, edited by L. Bjørnø (IPC Science and Technology, Guiedford, England, 1974), p. 168] also calculated the decay of ultrasonic waves in nonlinear media. Instead of the amplitude loss equation, they start with the energy equation

$$dI_1(x)/dx = -2\alpha I_1(x) - KG(x) I_1^2(x) \ ,$$

where $I(x)$ is the intensity of the wave, $K = \beta^2\omega^2/\rho_0 c_0^5$ and $G(x) = (1 - e^{-2\alpha x})/2\alpha$ for a plane wave. The characteristic of this equation is different from Eq. (2); i.e., the equation considers the loss due to the interaction between the fundamental wave and the second harmonic to generate the third harmonic, but does not take into account the loss due to the generation of the second harmonic itself. The resulting solution was found not to fit our data.
[11]H. Kwun, A. Hikata, and C. Elbaum, J. Low Temp. Phys. (in press).
[12]K. R. Atkins and R. A. Stasior, Can. J. Phys. 31, 1156 (1953).
[13]J. Wilks, *The Properties of Liquid and Solid Helium* (Clarendon, Oxford, 1967).
[14]J. Lighthill, J. Sound Vib. 61, 391 (1978), and references cited therein.
[15]R. D. Finch, R. Kagiwada, M. Barmatz, and I. Rudnick, Phys. Rev. 134, A1425 (1964); T. Vroulis, E. A. Neppiras, and R. D. Finch, J. Acoust. Soc. Am. 59, 255 (1976).

[16]A. V. Granato and K. Lücke, J. Appl. Phys. 27, 583 (1956).
[17]A. Hikata and C. Elbaum, Phys. Rev. Lett. 18, 750 (1967).
[18]A. Hikata, J. Deputat, and C. Elbaum, Phys. Rev. B 6, 4008 (1972); A. Hikata and C. Elbaum, *ibid.* 9, 4529 (1974).
[19]Y. M. Gupta, A. Hikata, and C. Elbaum, Scr. Metall. 11, 249 (1977).
[20]The cause of the persistent $\Delta\alpha$ is not clear at present. Experiments to investigate this phenomenon are in progress.
[21]R. Cline, Ph.D. thesis (Brown University, 1979) (unpublished).
[22]I. Iwasa and H. Suzuki, Proceedings of the 3rd International Conference on Phonon Scattering in Condensed Matter, Providence, Rhode Island, 1979 (in press).
[23]I. Iwasa (private communication).
[24]See, for example, J. Friedel, in *Proceedings of the Symposium on The Interaction between Dislocations and Point Defects,* edited by B. L. Eyer (Atomic Energy Research Establishment, R5944, Harwell, England, 1968), Vol. I, p. 1; M. Meshii, *ibid.*, Vol. III, p. 566.
[25]A. Hikata, B. B. Chick, and C. Elbaum, Appl. Phys. Lett. 3, 195 (1963); A. Hikata and C. Elbaum, Phys. Rev. 144, 469 (1966); 151, 442 (1966); I. F. Mirsayev, V. V. Nikolayev, and G. G. Taluts, Phys. Met. Metallogr. (USSR) 31, 6 (1971); I. F. Mirsayev, *ibid.* 38, 208 (1974).
[26]See, for example, F. R. N. Nabarro, *Theory of Crystal Dislocations* (Clarendon, Oxford, 1967).
[27]D. J. Sanders, H. Kwun, A. Hikata, and C. Elbaum, Phys. Rev. Lett. 39, 815 (1977); 40, 458 (1978).
[28]K. Brugger, Phys. Rev. 133, A1611 (1964).
[29]R. D. Peters, M. A. Breazeale, and V. K. Pare, Phys. Rev. B 1, 3245 (1970).
[30]Y. Hiki and A. V. Granato, Phys. Rev. 144, 411 (1966).
[31]J. R. Drubble and R. E. Strathen, Proc. Phys. Soc. London 92, 1090 (1967).
[32]E. H. Bogardus, J. Appl. Phys. 36, 2504 (1965).
[33]T. Bateman, W. P. Mason, and H. J. McSkimin, J. Appl. Phys. 32, 928 (1961).
[34]H. J. McSkimin and P. Andreath, J. Appl. Phys. 35, 3312 (1964).
[35]J. E. Mackey and R. T. Arnold, J. Appl. Phys. 40, 4806 (1969).
[36]J. H. Cantrell, Jr., and M. A. Breazeale, Phys. Rev. B 17, 4864 (1978).
[37]F. Tsuruoka and Y. Hiki, Phys. Rev. B 20, 2702 (1979).
[38]A. F. Andreev, J. Phys. (Paris), Colloq. 39, C6-1257 (1978).
[39]R. A. Guyer, R. C. Richardson, and L. I. Zane, Rev. Mod. Phys. 43, 532 (1971).